Preprint of
Schmidt, A. 2001. Visualisation of multi-source archaeological geophysics data.
In M. Cucarzi and P. Conti (eds) *Filtering, Optimisation and Modelling of Geophysical Data in Archaeological Prospecting*: 149-160. Rome: Fondazione Ing. Carlo M. Lerici.

See http://www.GeodataWIZ.com/armin-schmidt

Visualisation of Multi-Source Archaeological Prospection Data

by Armin Schmidt
Armin.R.Schmidt@Gmail.com

Abstract

The simultaneous use of several archaeological prospection techniques can provide additional information for the interpretation of buried features. For this to work, it is necessary to explore the spatial relation between the data sets and appropriate visualisation is required. Different data sets can be combined into a single compound that represents all data available, although the sources can no longer be differentiated. Using different visual classes (e.g. contour lines, grey shades, surfaces and orthogonal colours) allows to overcome these limitation. The various methods are evaluated with synthetic model data and field results from the Newstead Roman Fort.

Introduction

Buried archaeological sites are a precious part of the cultural heritage and their investigation or management should involve minimal damage or destruction. Geophysical methods are frequently used for detailed non-invasive investigations of such sites. They rely on the contrast of a buried feature to the surrounding soil in one or more of its physical properties that can be detected by surface measurements. The two most commonly used techniques are earth resistance (R) and magnetic field gradiometer (ΔB) measurements. Other techniques include the measurement of magnetic susceptibility, electromagnetic conductivity and vertical resistivity profiles. In addition, surface radar (GPR) surveys are becoming feasible.

Frequently, more than one technique is used to investigate a site; one reason being the difficulty to predict which method would yield best results, despite some heuristic rules based on geology, climate and archaeological context (David 1995, 9; Clark 1996, 124). A further reason is the additional information that can be gained from a comparison of results obtained with several methods since dissimilar archaeological features may manifest themselves differently in the various techniques. For example, a ditch is frequently characterised by a low resistance and a high magnetic anomaly whereas a foundation of granite stones may produce high resistance and high magnetic data. This approach is similar to the use of multi-spectral images in remote sensing where surface objects are meant to produce characteristic ‘fingerprints’ in the way they affect different spectral bands (Hord 1982, 96).

However, before such interpretation can be undertaken, data from different sources have to be visualised in an appropriate way. Most often this is simply done by displaying different data-plots side-by-side (see for example Figs. 1a and 1b; and Cole 1997, figure 4). The difficulty with this method is to relate the position of different anomalies accurately between the images. A better approach is using digital displaying techniques where an operator can easily flip between data from different sources on a computer screen thus ‘remembering’ the location of areas of interest. However, publishing such display in conventional static formats is not possible.

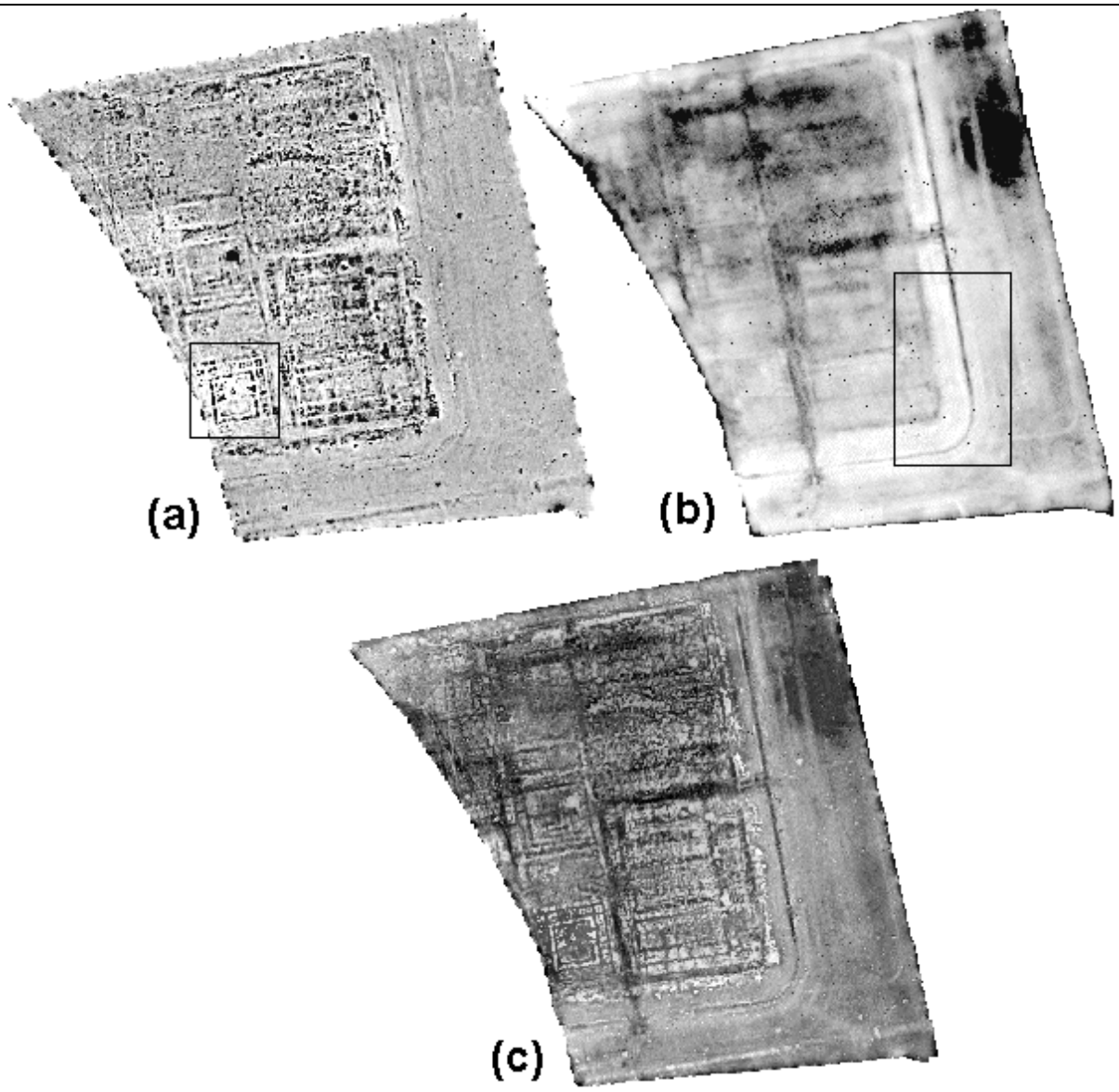

Figure 1: Geophysical surveys at Newstead Roman Fort, UK. The diagrams are aligned with north to the top and overall dimensions of the plots are 340m ×300m. (a) Fluxgate gradiometer data (ΔB), -6...+6nT (white to black, linear), (b) earth resistance data (R), 59...109Ω (white to black, linear) and (c) combination of the scaled data sets R'- ΔB' (see text). The outlines indicate the areas investigated further.

This paper investigates the possibilities of advanced visualisation of multi-source archaeological prospection data as still images. Various methods are explored including the combination of data into a single new layer and the use of visual classes to distinguish data from different sources. In order to demonstrate the various techniques, synthetic and field data of earth resistance and fluxgate gradiometer measurements are used (Schmidt 1996). It should be born in mind that the preparation of data for visualisation will also be the first stage for any automatic classification or interpretation algorithm that may be developed.

The Nature of Geophysical Data

In remote sensing (satellite imagery or aerial photography) each recorded data value (pixel) can uniquely be associated with an area on the ground surface from which the electromagnetic radiation was emitted. This is due to the fact that only the topmost part of the ground or vegetation is emitting radiation. As a consequence, it is possible to treat each data point individually without considering

any of its neighbours. In contrast, geophysical measurements depend on all material properties in a considerable subsurface volume, surrounding the measurement location. This implies that neighbouring measurements are affected by the same subsurface elements which gives rise to complex geophysical responses and makes the immediate association of measurements and buried features difficult. In addition, the response characteristics of the various geophysical techniques are very different and have to be taken into account when attempting a combined visualisation.

To examine the problems involved, earth resistance data were calculated for a twin-electrode array passing longitudinally over a buried insulating sphere with radius 0.6203m and its centre at 0.75m depth using the analytical expressions derived by Lynam (1970, 64) for the response R/R_b where R_b is the background resistance (see Fig. 2a). Fluxgate gradiometer data (ΔB) were calculated for a buried cube[†] of the same volume (i.e. side length 1m) and same depth of centre according to Sheen and Aspinall (1997) (see Fig. 2b). The magnetisation of the cube was assumed to be entirely induced with an inclination of the earth's magnetic field of 70°N and an arbitrarily scaled positive susceptibility contrast. While figure 2 only shows single trace, both data sets were calculated on a regular two-dimensional grid with a node separation of 0.2m. It is clear from the comparison in figure 2 that the shape of the anomalies is different (the magnetic anomaly having a negative trough to the north). In addition, the positions of the maxima are offset against each other and against the location of the buried feature. Such differences have to be taken into account when comparing or combining data obtained with different techniques. Cammarano *et al.* (1997) suggest that all data should be converted to a common measure of "feature probability" which would involve an inversion of data and may be computationally difficult. However, it may be concluded from figure 2 that earth resistance data could be used as recorded in the field and magnetometer data only need shifting of the maxima towards the centre of the buried features. The reduction-to-the-pole operator (Baranov 1957, Tabbagh *et al.* 1997) can be used to achieve such a transformation. This processing will only lead to a noticeable shift of the recorded maxima if the sampling interval of the acquired field data is fine enough. It is hence important to adjust the processing to the actual needs of the available data set.

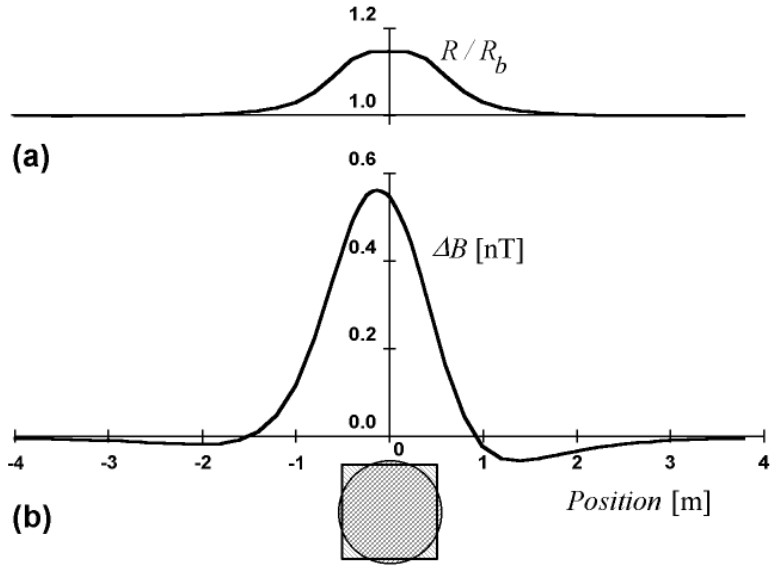

Figure 2: Calculated responses across the centre of the models described in the text. (a) Earth resistance anomaly of sphere and (b) magnetic field gradiometer anomaly of a prism.

[†] Sphere and cube were chosen since they are the most appropriate objects for analytical calculations of earth resistance and magnetometer anomalies, respectively.

In addition to the synthetic data mentioned, field results will be used for the discussion of geophysical pre-processing and visualisation techniques. Earth resistance and fluxgate gradiometer data were measured on the site of the Newstead Roman Fort (near Melrose, Borders Region, UK, Figs. 1a and 1b). Earth resistance was measured with a twin-electrode resistance array (probe spacing 0.5m) and the RM15 earth resistance meter. Magnetometer data were recorded with the FM36 fluxgate gradiometer. Both data sets were obtained with a spatial resolution of 1m × 1m. Indicated in figure 1 are two areas that will be investigated in more detail. The 'Commander's House' in the SW had been excavated and backfilled earlier this century by James Curle (Curle 1911). In the SE, an area was selected that includes the wall with its inner rampart and an entrance gate.

Visualisation of Compounds

One way of visualising the spatial relationship between data sets is to derive a single compound set that represents the summary of the information. The obvious drawback of this approach is the difficulty to differentiate between the original data sources once they have been merged. According to the number of neighbouring data values in the vicinity of an investigated location that are used to derive a single new value one can distinguish between local and focal compounds (Tomlin 1990, 96). Such compounds can then be displayed in the usual way using, for example, greyscale or contour diagrams.

Local Compounds

If only local correlation between data is of interest a new data set may be derived by combining those data from various sources that were recorded at the same position to yield a value for the compound set. A simple, though effective, method is to adjust the range of values in all data sets such that they are comparable before combining them. Data values can be scaled by stretching a certain range onto a common interval of, for example, 0 to 1 or 0 to 256. It was found that best results are achieved if only data within the 5- and 95-percentile range of the total histogram are used. The compound data will contain all features that are visible in any single set. Care has to be taken to enhance, rather than extinct, features that are recorded by several techniques. For example, buried ditches often show a positive magnetic responses but low earth resistance. In contrast, stone foundations may have positive magnetic and high resistance signatures. Depending on the prevailing features on a site the appropriate mathematical combination of data has to be chosen. For the Newstead Roman Fort most foundations seem to produce negative magnetic and high resistance anomalies. In figure 1c this has been taken into account by forming the difference $R' - \Delta B'$ where $\Delta B'$ and R' are the scaled data sets. It is apparent that a very satisfactory representation of all features on the site has been achieved but discrimination of the data source is no longer possible. It was demonstrated by Neubauer and Eder-Hinterleitner (1997) that local compounds calculated from the multiplication of scaled data can also provide useful aids for interpretation.

Focal Compounds

It was mentioned earlier that the relationship between geophysical data values and the location of buried features is complex. Therefore, the calculation of local compounds, that seem most appropriate for remotely sensed data, may have to be amended to obtain more indicative results. Focal compounds are derived by taking a neighbourhood into account that surrounds an investigated position when calculating a single new value (Tomlin 1990, 96). An example for a focal compound is the calculation of a correlation coefficient.

In order to test any two data sets for similar trends they can be statistically analysed. Figure 3 is a scatterplot of the synthetic magnetometer data *vs.* the earth resistance data. Such diagram does not show the spatial position of each data point but indicates the relationship between the two data sets.

The loop visible is due to the shift of the peak in the magnetometer data. The correlation coefficient *r* calculated for the two data sets is a statistical measure of their similarity. Values with modulus near 1 indicate strong correlation (i.e. both data sets show a similar trend): if data peak in the same direction $r \approx 1$, if they peak in opposite directions $r \approx -1$. The synthetic data sets have a correlation coefficient of 0.958. When the synthetic magnetometer data are reduced to the pole the 'loop' in figure 3 closes and the correlation becomes very high (0.992). This approach can be extended to analyse data from a two-dimensional neighbourhood for their similarity and assign the corresponding correlation coefficient to the centre of such neighbourhood (Fig. 4). The correlation results for the data from Newstead Roman Fort (Fig. 5a), after reduction to the pole, appear mottled. A positive correlation can be found on the line of the Eastern wall (positive magnetic and low earth resistance data) and the internal street system shows some negative correlation (negative magnetic and positive earth resistance data). It is possible that the buildings burnt down producing a negative susceptibility contrast between the burnt soil and the stone foundations.

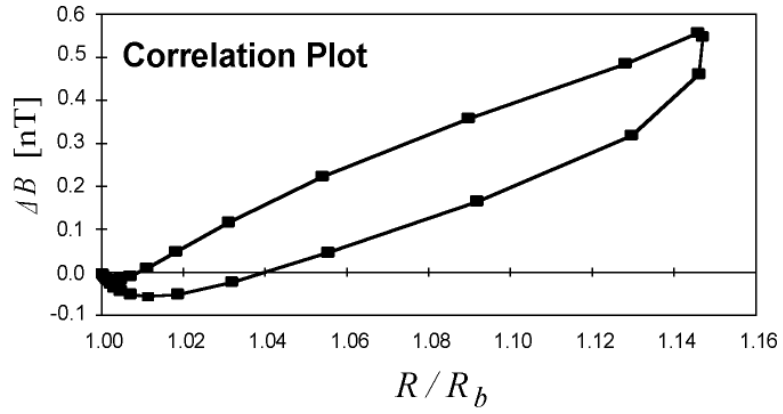

Figure 3: Scatterplot of magnetometer (ΔB) vs. earth resistance data (R/R_b) for the models used.

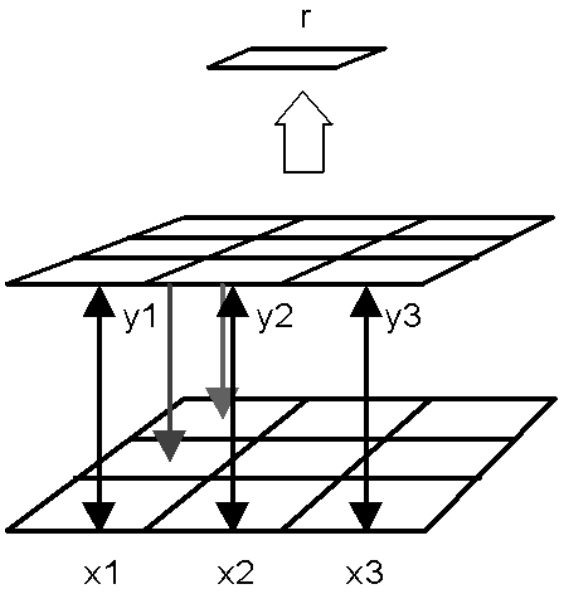

Figure 4: Calculation of correlation coefficient r(x,y) for a two-dimensional neighbourhood.

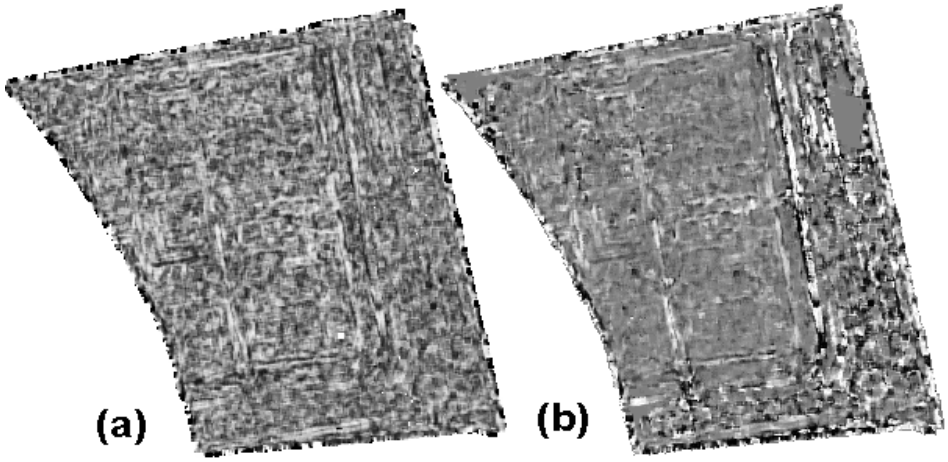

Figure 5: Correlation analysis for Newstead Roman Fort after reduction to the pole. (a) Correlation within a 4m wide neighbourhood, -1...+1 (white to black, linear) and (b) linear regression coefficient within the neighbourhood, arbitrary units (white to black, linear).

Correlation coefficients will be close to 1 if both data sets show no anomaly and also if an anomaly in one data set is much bigger than in the other, giving rise to some background noise. To overcome this limitation, the regression coefficient (corresponding to the slope of a regression line in figure 3) of the data in a neighbourhood can be plotted in a focal compound. Figure 5b shows the results for the survey data which indicates the features with positive and negative correlations more clearly. It is apparent that no correlation can be seen for the Commander's House (see below) but a weak correlation is visible for the Headquarters to the North of it.

Visual Classes

For an advanced interpretation of geophysical data from multiple sources it is often necessary to refer to the spatial relationship and the anomaly-shape of individual data sets. As mentioned before, this cannot be accomplished if data are fused into a compound. To display several data sets simultaneously and retain their distinction, visual classes can be used. A visual class can be defined as any visual category that may be distinguished in a display by a human observer. Examples include contour lines, grey or colour shades, topographic heights, and 'orthogonal colour components'. The combination of these visual classes for the display of multi-source data is discussed in the following sections.

Contours

If contour lines of one data set are overlain over a grey or colour shade plot of another data set, the two can easily be distinguished by an observer as two different visual classes. This can be used to investigate the spatial relationship between two geophysical data sets. To keep such display simple, it is advisable to use smoothly varying data for the contour lines. It is therefore possible to draw earth resistance data as contour lines over a grey or colour shade plot of magnetometer data. The result of such combination for the synthetic data (Fig. 6a) clearly shows the shift of the magnetometer peak against the earth resistance maximum.

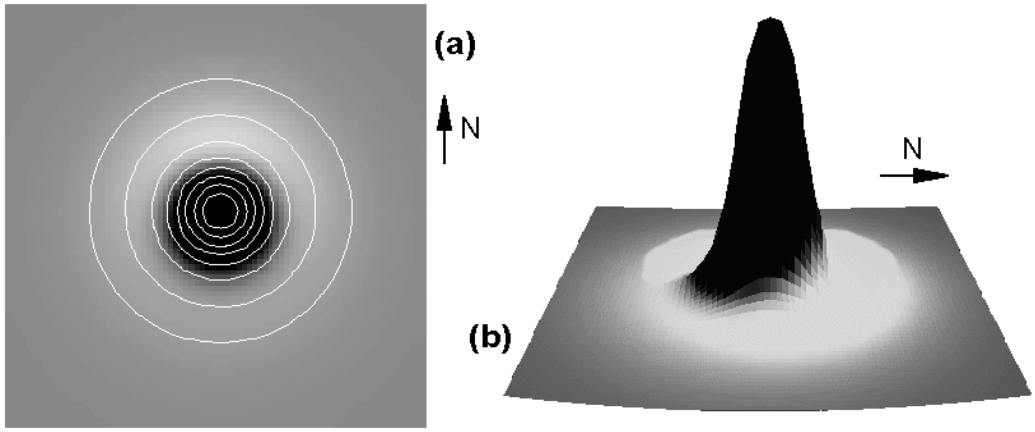

Figure 6: Use of visual classes to display the relationship between ΔB and R data for the models discussed. (a) Contour lines of R over grey shades of ΔB and (b) grey shades of ΔB draped over a surface defined by R.

Topography

Contour lines are commonly used to display topographic heights in two dimensions; either on paper or on a computer screen. However, advances in computer visualisation have led to algorithms that allow realistic visualisation of three-dimensional surfaces on such two-dimensional media (Foley *et al.* 1994, 195). Hence, the concept of contour lines as visual class can be extended to visualise one data set (e.g. earth resistance) as a topographical surface and using grey or colour shading of the created 'landscape' as second visual class for a different data set. Such display of a three-dimensional topography coloured according to another data set is sometimes referred to as 'four-dimensional'. This concept is illustrated for the synthetic data in figure 6b.

The technique was applied to the two selected areas of the Newstead Roman Fort (Fig. 7), earth resistance measurements being used to form a topographical landscape and magnetic field gradiometer data draped over it as a greyscale image. In figure 7a the Commander's house is situated in a 'valley' of relatively constant low resistance and only the magnetometer data indicate the presence of the structural remains, albeit very clearly. It may be concluded that the absence of any earth resistance anomalies is due to the earlier excavation and only the magnetic measurements were able to detect the deeper undisturbed foundations. As mentioned above the foundations show as negative magnetic anomalies. The negative susceptibility contrast, responsible for it, may be caused by burnt soil filled in between the foundations. The SE corner of the wall (Fig. 7b) shows that most of the magnetic anomalies lie inside the fort, away from the rampart, which is characterised by a band of low resistance. However, one pronounced magnetic anomaly can be seen to cut into the low-resistance feature and may be interpreted as a hearth or oven built *into* the rampart. This archaeologically important conclusion can only be deferred from the detailed spatial analysis of the multi-source data.

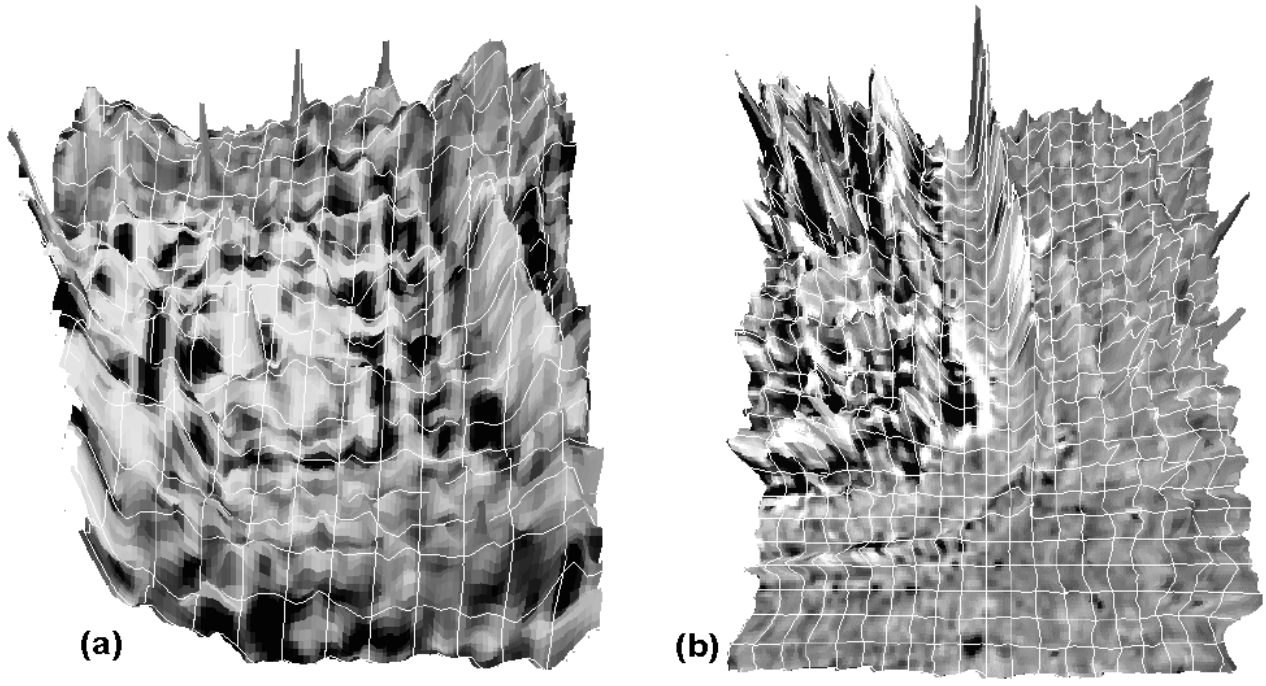

Figure 7: Visualisation of geophysical data from Newstead Roman Fort as grey shades of ΔB draped over a surface defined by R. (a) Commander's house and (b) SE corner of the wall.

Colour

The three base colours red, green and blue can be termed 'orthogonal' since any other colour can be uniquely composed from a linear intensity combination (Foley *et al.* 1994, 410). This forms the principle of modern colour screens as used in TV and computer units. The orthogonality can be visualised as a colour cube (Fig. 8) where each base colour represents an axis in a three-dimensional colour-space thus allowing to associate each possible colour with the intensities of the three base colours. This principle has been used to produce false-colour images of multispectral remotely sensed data by associating each data set with one base colour (Williams 1995, 57). A skilled human interpreter is able to estimate the contribution of each data set to the overall colour image. In this respect the orthogonal colours may be referred to as visual classes.

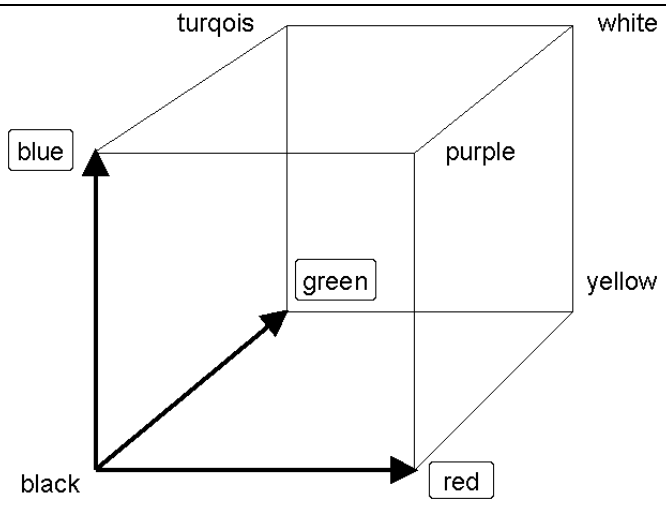

Figure 8: Colour cube formed by three base colours.

Obviously, the same concept can be applied to multi-source archaeological prospection data. In order to simplify the interpretation, however, the analysis may be restricted to only two data sources. Since magnetic gradiometer data have a defined zero-level their positive and negative values, which

are both indicative for the interpreter, may be mapped to a separate colour component (Aspinall and Haigh 1988). A third colour component may then be used to represent earth resistance. Using the widest span of the orthogonal colours may result in a scheme as indicated in figure 9a where positive and negative magnetic values are represented as red and blue respectively ('y-axis') and earth resistance is associated to green ('x-axis'). Such scheme was suggested by Schmidt (1996) and Eder-Hinterleitner (1997). However, data sets visualised according to this scheme suffer from the representation of high resistance data by bright green, despite being usually associated with dry soil,. A more appropriate coding of high resistance as yellow (Fig. 9b) proved to be beneficial for the training of interpreters. The loss of quantitative resolution between the colours is far outweighed by the clarity of representation. If the distinction between positive and negative gradiometer data is not required, a two-dimensional colour scheme (e.g. only red and blue) can be used to represent two data sets (Orbons 1998).

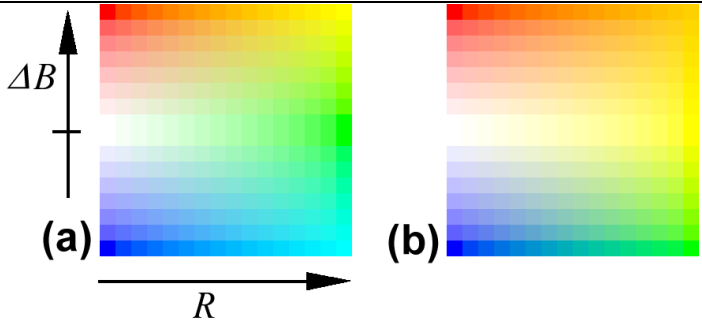

Figure 9: Colour wedges of ΔB (y axis) vs. R (x axis) data. (a) High resistance can be represented as green or (b) as yellow.

Figure 10 shows the colour coding of the synthetic data. The shift of the magnetometer peak produces very characteristic colour fringes (Fig. 10a) that can be used to clearly identify the spatial relationships of the maxima in the two data sets. As expected, the fringes disappear after reduction to the pole (Fig. 10b).

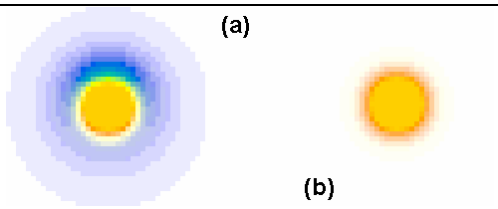

Figure 10: Calculated model data (ΔB and R) displayed with the yellow colour wedge. (a) Raw gradiometer data and (b) after reduction of the pole.

When the Newstead Roman Fort data were subjected to such colour display (Fig. 11) the features discussed for the topographical presentation above, could be identified with ease. The wall (Fig. 11b) shows mainly yellow to the east, due to a lack of magnetic signals, while it becomes more orange and green to the south, indicating weak magnetic anomalies at these positions. There are several magnetic anomalies on the rampart indicated by a clear red/blue signature of their response (i.e. low earth resistance). Inside the fort, all magnetic anomalies are orange and green due to the higher resistance there. Reduction to the pole (Fig. 11c) reduced the extent of the magnetic anomalies' negative parts but made little difference to the interpretation of the features. This is due to the sampling interval being similar to the features investigated.

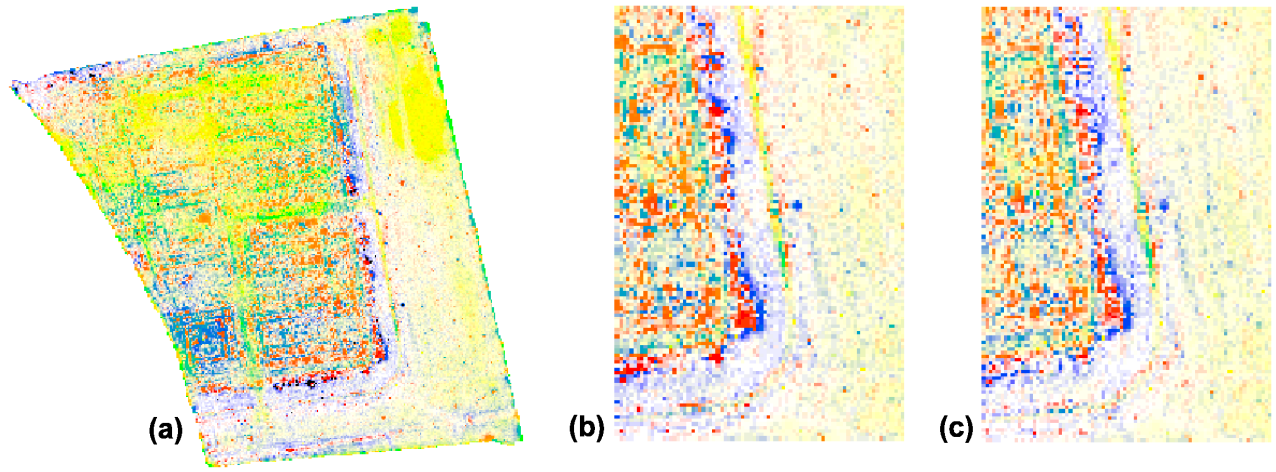

Figure 11: Geophysical data from Newstead Roman Fort (ΔB and R) displayed with the yellow colour wedge. (a) Full survey area, (b) SE corner of the wall and (c) after reduction of the pole.

Conclusions

It has been shown that various techniques are available for the visualisation of multi-source archaeological prospection data. Using compounds allows a quick overview of all anomalies present (local compounds) or a statistical analysis of the relationship between the data (focal compounds). While this can be very useful for a first assessment of results, a detailed analysis is not possible since different data sources can not be distinguished. This is overcome by the use of distinct visual classes to display two or more data sets simultaneously in their spatial relationship. Three different methods have been presented here and have been evaluated with synthetic and field data.

The use of contour lines on grey-scale plots is a technique that is easy to implement. However, several points have to be noted. If contour lines are becoming very dense (e.g. due to strong changes associated with shallow features) an underlying grey-scale plot may be difficult to see. If contour labels are omitted to overcome this problem, the well-known ambiguity of contour plots between positive and negative gradients may cause difficulties in the interpretation. However, if the data set that is represented by contour lines varies gradually and smoothly across the display area, very satisfactory results can be obtained.

Extending this approach into four-dimensional surface displays can overcome the aforementioned ambiguity but the selection of an appropriate viewpoint for the scene is subjective and time consuming, even with modern computing facilities.

Independent colours for the simultaneous representation of data sets has proved successful in remote sensing applications (Drury 1998, 94) and has been demonstrated for archaeological prospection in this work. While interpretation of such displays requires training of the interpreters, it can lead to very clear representations of the relationship between data sets, as was illustrated for data from the Newstead Roman Fort. The quality of modern colour computer screens allows a good distinction of colour shades in the diagrams. Printed reproduction requires good quality colour printing to achieve the desired results.

It is difficult to make general statements about the best procedure for dealing with multi-source prospection data. For a first assessment data compounds provide a quick overview that can highlight areas of interest that should then be investigated with a combination of other methods, mentioned in the text. The clarity of results that can be achieved with multi-colour data plots makes them very suited.

It has been demonstrated that the need for pre-processing depends on the spatial resolution of the data. For closely sampled data (see the results for the synthetic data sets) a reduction to the pole can improve results considerably (see Fig. 10). However, if for a reconnaissance survey the sampling interval lies in the order of the feature dimensions (see the results for the Newstead Roman Fort) such processing makes only little difference.

Acknowledgements

The author would like to thank Dr. Rick Jones and Paul Cheetham for the provision of the geophysical data from the Newstead Roman Fort. Brett Scaife and Nic Sheen implemented the software for the analytical expressions for earth resistance and fluxgate gradiometer anomalies, respectively.

Bibliography

Aspinall, A. and High J.G.B., 1988. A review of techniques for the graphical display of geophysical data. In: S.P.Q. Rahtz (ed.), *Computer and Quantitive Methods in Archaeology 1988*, BAR International Series 446(ii), Tempus Reparatum, Oxford, pp. 295-307.

Baranov, V., 1957. A new method for interpretation of aeromagnetic maps: pseudo-gravimetric anomalies. *Geophysics*, 22: 359-383.

Cammarano, F., Piro, S., Rosso, F. and Mauriello, P., 1997. High resolution geophysical prospecting with integrated methods: The case of ancient acropolis of Veio (Rome, Italy). *Annales Geophysicae*, 15, Suppl. I: C87.

Clark, A., 1996. *Seeing Beneath the Soil, Prospecting methods in archaeology*, 2nd ed. Batsford, London.

Cole, M., 1997. Geophysical Surveys of Three Pond Barrows in the Lake Down Barrow Group near Wilsford, Wiltshire. *Archaeological Prospection*, 4: 113-121.

Curle, J., 1911. *A Roman Frontier Post and its People. The Fort at Newstead*.

David, A., 1995. *Geophysical survey in archaeological field evaluation*. English Heritage Research and Professional Services Guideline, Vol. 1. English Heritage, London.

Drury, S.A., 1998, *Images of the Earth*, 2nd edition. Oxford University Press, Oxford.

Foley, J.D., van Dam, A., Feiner, S.K., Hughes, J.F. and Phillips, R.L., 1994, *Introduction to Computer Graphics*, Addison-Wesley, Reading.

Hord, R.M., 1982. *Digital Image Processing of Remotely Sensed Data*. Academic Press, New York.

Lynam, J.T., 1970. *Techniques of geophysical prospection as applied to near surface structure determination*. Ph.D. Thesis submitted to the Department of Physics, University of Bradford, U.K.

Neubauer, W. and Eder-Hinterleitner, A. (1997), Resistivity and Magnetics of the Roman Town Carnuntum, Austria: An Example of Combined Interpretation of Prospection Data, *Archaeological Prospection*, 4: 179-189.

Orbons, P.J., 1998. Geophysical Support in Large Scale Archaeological Prospections, Recent Case-Studies and Research. *Annales Geophysicae*, 16, Suppl. I: C227.

Schmidt, A., 1996. Visualisation of multi-source archaeological geophysics data. *Annales Geophysicae*, 14, Suppl. I: C165.

Sheen, N.P. and Aspinall, A., 1995. A simulation of anomalies to aid the interpretation of magnetic data. In: J. Wilcock and K. Lockyear (eds.), *Computer Applications and Quantitative Methods in Archaeology 1993*. BAR International Series 598, Tempus Reparatum, Oxford, pp. 57-63.

Tabbagh, A., Desvignes, G. and Dabas, M., 1997. Processing of Z gradiometer magnetic data using linear transforms and Analytical Signal. *Archaeological Prospection*, 4: 1-14.

Tomlin, C.D., 1990. *Geographic information systems and cartographic modeling*. Prentice-Hall, Inc., New Jersey.

Williams, J. 1995. *Geographic Information from Space: processing and applications of geocoded satellite images*. John Wiley & Sons, Chichester.